Biochemistry

pubs.acs.org/biochemistry
Article

Functional Characterization of Two Polymerizing Glycosyltransferases for the Addition of *N*-Acetyl-D-galactosamine to the Capsular Polysaccharide of *Campylobacter jejuni*

Dao Feng Xiang, Tamari Narindoshvili, and Frank M. Raushel*

Cite This: *Biochemistry* 2025, 64, 591−599
Read Online

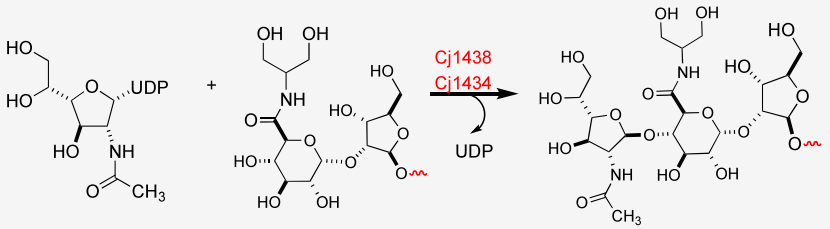

ABSTRACT: The exterior surface of the human pathogen *Campylobacter jejuni* is coated with a capsular polysaccharide (CPS) that consists of a repeating sequence of 2−5 different sugars that can be modified with various molecular decorations. In the HS:2 serotype from strain NCTC 11168, the repeating unit within the CPS is composed of D-ribose, *N*-acetyl-D-galactosamine, and a D-glucuronic acid that is further amidated with either serinol or ethanolamine. The D-glucuronic acid moiety is also decorated with D-glycero-L-gluco-heptose. Here, we show that two different GT2 glycosyltransferases catalyze the transfer of *N*-acetyl-D-galactosamine from UDP-NAc-D-galactosamine furanoside to the C4-hydroxyl group of the D-glucuronamide moiety at the growing end of the capsular polysaccharide chain. Catalytic activity was not observed with glycosides of D-glucuronic acid, and thus, the C6-carboxylate of the D-glucuronic acid moiety must be amidated prior to chain elongation. One of these enzymes comprises the N-terminal domain of Cj1438 (residues 1−325) and the other is from the N-terminal domain of Cj1434 (residues 1−327). These two glycosyltransferases are ∼87% identical in sequence, but it is not clear why there are two glycosyltransferases from the same gene cluster that apparently catalyze the same reaction. This discovery represents the second polymerizing glycosyltransferase that has been isolated and functionally characterized for the biosynthesis of the capsular polysaccharide in the HS:2 serotype of *C. jejuni*.

INTRODUCTION

Campylobacter jejuni is an important human pathogen regarded as a major causative agent of bacterial gastroenteritis. The symptoms of *C. jejuni* infection typically include fever, nausea and abdominal cramping, and bloody diarrhea.[1] Additionally, campylobacteriosis can result in myocarditis, irritable bowel syndrome, and Guillain-Barré Syndrome.[2−4] *C. jejuni* is transmitted to humans from animals, primarily chickens, where *C. jejuni* is part of the normal intestinal microbiota, but can also be transmitted from cattle, pigs, sheep, and domestic cats and dogs.[5,6] Currently, there are no FDA-approved vaccines for the prevention of a *Campylobacter* infection. So far, the best candidates are vaccine conjugates, which mimic the surface exposed capsular polysaccharides (CPSs).[7] The CPS protects bacteria from desiccation and from complement mediated phagocytosis.[8] Additionally, the CPS of *C. jejuni* plays an important role in colonization and invasion of the host immune system.[9]

The structure of the repeating CPS unit from *C. jejuni* NCTC 11168 (serotype HS:2) is illustrated in Figure 1 and is composed of D-ribose (D-Rib), *N*-acetyl-D-galactosamine (D-Gal*f*NAc), D-glucuronic acid (D-GlcA), and D-*glycero*-L-*gluco*-heptose.[10] We and others have previously elucidated the biosynthetic pathways for some of the activated carbohydrates that are presumably used as sugar donors during the polymerization of this CPS.[10−39] These include GDP-D-*glycero*-L-*gluco*-heptose, UDP-D-glucuronic acid (UDP-GlcA), and the furanose form of UDP-Gal*f*NAc.[18,21−24] Previously, we identified and characterized the first enzyme (Cj1432) shown to catalyze the formation of the glycosidic bond between D-ribose and D-glucuronic acid using methyl-*β*-D-riboside as the acceptor substrate and UDP-GlcA as the sugar donor substrate.[40] In this investigation, we have identified two additional enzymes (Cj1438 and Cj1434) that catalyze the formation of the glycosidic bond between *N*-acetyl-D-glucosamine and the D-glucuronic acid moiety during the polymerization of the CPS from the HS:2 serotype of *C. jejuni*.

Received: October 18, 2024
Revised: January 2, 2025
Accepted: January 10, 2025
Published: January 24, 2025

https://doi.org/10.1021/acs.biochem.4c00704
Biochemistry 2025, 64, 591−599

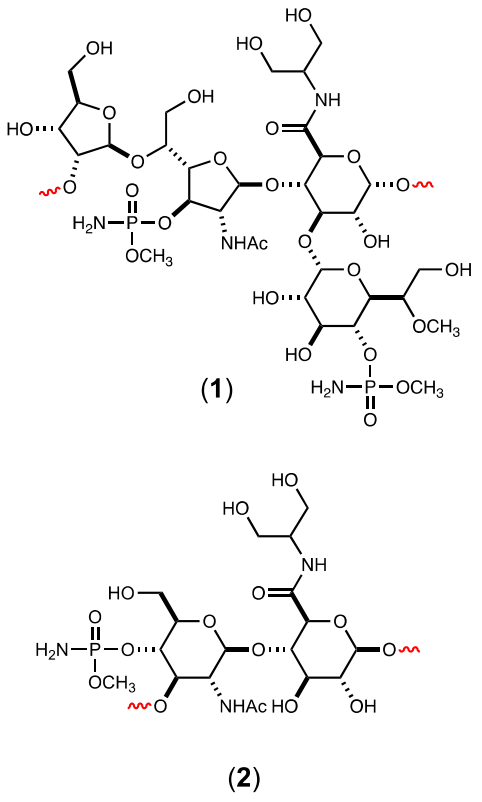

Figure 1. Structures of the repeating polysaccharides found in the CPS of the HS:2 serotype of *C. jejuni* strain NCTC 11168 (**1**) and the HS:19 serotype of *C. jejuni* strain NCTC 12517 (**2**).[10,13,14] The glucuronic acid moiety in the HS:2 serotype can also be amidated with ethanolamine.[37]

MATERIALS AND METHODS

Materials. Lysogeny broth (LB) and isopropyl-β-D-thiogalactopyranoside (IPTG) were purchased from Research Products International. HisTrap columns, HiTrap Q HP anion exchange columns, and Vivaspin 20 10 kDa MWCO spin filters were obtained from Cytiva. The 10K Nanosep spin filters were purchased from PALL Corp. (Port Washington, NY). All other materials and chemicals were purchased from Sigma-Aldrich, GE Healthcare, Bio-Sciences, or Carbosynth, unless otherwise stated.

Synthesis of Potential Substrates for Cj1438$_N$ and Cj1434$_N$. Chemical syntheses of compounds **3**−**7** are described in the Supporting Information. The enzymatic syntheses of compounds **10a** and **10b** have been described previously.[40] The structures of these compounds and other enzymatically formed products are listed in Figure 2.

Cloning, Expression, and Purification of Cj1438$_N$. The gene encoding the N-terminal domain (residues 1−325) of Cj1438 (UniProt id: Q0P8H6) from *C. jejuni* NCTC 11168 genomic DNA (ATCC 700819D-5) was purchased from Twist Biosciences in a pET28a expression vector with an N-terminal hexa-histidine tag. The purified protein is designated as Cj1438$_N$ for this investigation. This construct was used to transform *Eschericha coli* BL21(DE3) competent cells, and single colonies were used to create starter cultures that contained kanamycin (50 μg/mL). The starter cultures were used to inoculate 1.0 L of LB. The cultures were allowed to grow at 37 °C until an OD_{600} of 0.6−0.8 was reached, and protein expression was induced by the addition of 1.0 mM IPTG. The cultures were grown at 20 °C for 18 h and then harvested by centrifugation (7000 rcf, 4 °C, 10 min). The resulting cell pellet was flash frozen in liquid nitrogen and stored at −80 °C. For purification of Cj1438$_N$, 10 g of frozen cells was resuspended in 100 mL of 50 mM HEPES, 300 mM KCl, 10 mM imidazole, pH 8.0, containing 0.05 mg/mL of a protease inhibitor cocktail and 40 U/mL of DNase I. The resuspended cells were lysed by sonication (QSONICA Sonicator Ultrasonic Processor) in an ice bath. The lysate was clarified by centrifugation at 18,000 rcf at 4 °C for 30 min. The clarified supernatant fluid was passed through a 0.45 μm syringe filter (Whatman) and then loaded onto a 5 mL HisTrap column (GE Healthcare) attached to an NGC liquid chromatography system (BioRad) previously calibrated with binding buffer (50 mM HEPES, 300 mM KCl, and 10 mM imidazole, pH 8.0). The His-tagged protein was eluted with a 0−50% gradient of elution buffer (50 mM HEPES, 0.25 M KCl, and 0.50 M imidazole, pH 8.0). The fractions containing the desired protein, as identified by sodium dodecyl sulfate (SDS) gel electrophoresis, were combined, and the imidazole was removed from the protein solution by dialysis using a buffer containing 50 mM HEPES and 250 mM KCl, pH 8.0. The protein was concentrated to ∼10 mg/mL, aliquoted, frozen in liquid nitrogen, and stored at −80 °C. The concentration of the protein was determined spectrophotometrically using a computationally derived molar absorption extinction coefficient at 280 nm.[41] The values of ε_{280} and molecular weight used for Cj1438$_N$ were 43,130 M^{-1} cm^{-1} and 40,648 Da, respectively. About 47 mg of protein was obtained per liter of cell culture. The amino acid sequence of the purified protein is presented in Figure S1.

Cloning, Expression, and Purification of Cj1434$_N$. The gene encoding Cj1434 (UniProt ID: Q0P8I0) from *C. jejuni* NCTC 11168 was truncated (residues 1−327) and purchased from Twist Biosciences in a pET28a expression vector with an N-terminal hexa-histidine tag. The isolated protein is designated as Cj1434$_N$ for this study. The plasmid containing the gene for Cj1434$_N$ was transformed in *E. coli* BL21(DE3) competent cells. The conditions for expression and purification of Cj1434$_N$ were the same as that for Cj1438$_N$. The fractions eluted from the HisTrap column were pooled based on the SDS gel analysis results, concentrated to ∼3 mg/mL after the imidazole was removed by dialysis in 50 mM HEPES, 250 mM KCl, pH 8.0, frozen in liquid N_2, and stored at −80 °C. The concentration of Cj1434$_N$ was determined spectrophotometrically using a computationally derived molar absorption extinction coefficient at 280 nm.[41] The values of ε_{280} and molecular weight used for Cj1434$_N$ were 50,200 M^{-1} cm^{-1} and 41,035 Da, respectively. Approximately 22 mg of protein was isolated per liter of cell culture. The sequence of the purified protein is presented in Figure S1.

Prediction of Three-Dimensional Structures of Cj1438$_N$ and Cj1434$_N$. The predicted three-dimensional structures of the full-length proteins, Cj1438 (AF-Q0P8H6−F1-v4) and Cj1434 (AF-Q0P8I0−F1-v4), were obtained from the AlphaFold database (https://alphfold.ebi.ac.uk).[42] From these structural models, the predicted domain interfaces were used to help identify the truncation sites for the expression of soluble and presumably functionally active forms of the glycosyltransferases embedded within these multidomain proteins.

Reactions Catalyzed by Cj1438$_N$ and Cj1434$_N$. The catalytic activities of Cj1438$_N$ and Cj1434$_N$ were initially

https://doi.org/10.1021/acs.biochem.4c00704
Biochemistry 2025, 64, 591−599

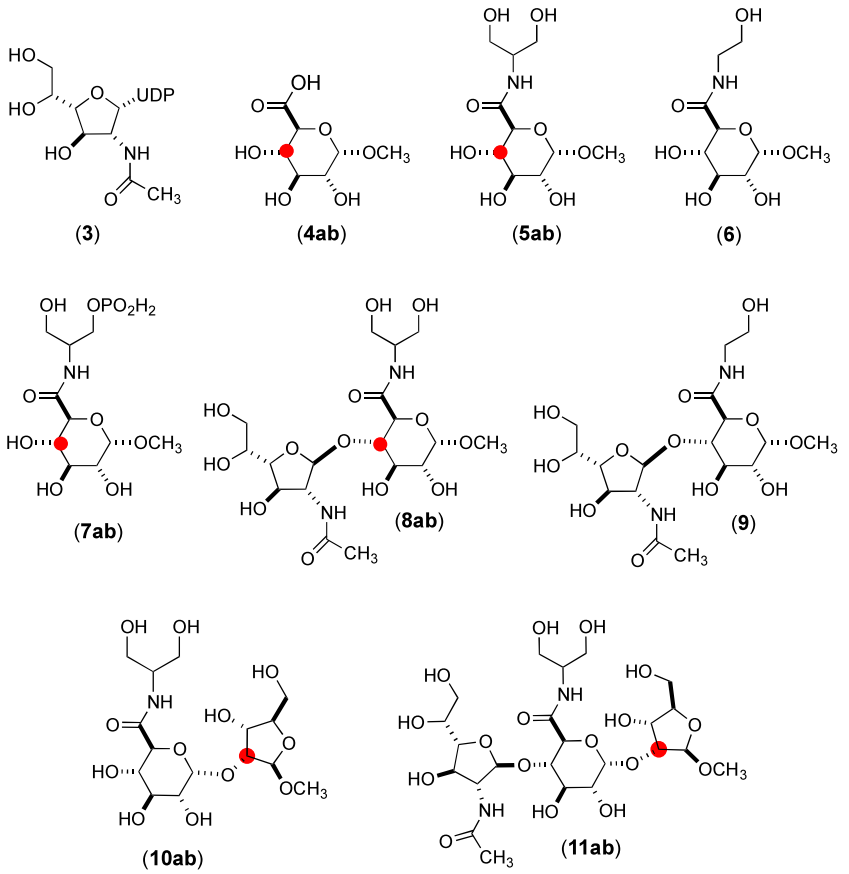

Figure 2. Structures of substrates and products produced for this investigation. The red dots in compounds **5**, **8**, **10**, and **11** represent a ^{13}C-label at the indicated carbon. In these structures, the compounds denoted with an "**a**" are the unlabeled compounds, whereas the compounds denoted with a "**b**" are the ^{13}C-labeled compounds.

investigated by adding the enzyme to 4.0 mM UDP-*N*-acetyl-D-glucosamine (**3**) with 3.0 mM potential acceptor substrates (compounds **4a**, **5a**, **6**, and **7a**). The reactions were conducted in 50 mM NH_4HCO_3, pH 8.0, 5.0 mM $MgCl_2$, and either 20 μM $Cj1438_N$ or $Cj1434_N$. The reaction mixtures were incubated at 25 °C overnight (~18 h). The protein was removed by using a 10K Nanosep spin filter (PALL) before product analysis by electrospray ionization (ESI)−mass spectrometry.

Identification of Reaction Products. The products of the reaction catalyzed by $Cj1438_N$ were investigated using ESI mass spectrometry in the positive ion mode. A 1.0 mL reaction mixture containing 20 μM $Cj1438_N$, 4.0 mM substrate **3**, and 3.0 mM compound **5a** was incubated at 25 °C overnight. The reaction mixture was passed through a 10K Nanosep spin filter (PALL) to remove the protein, diluted to 15 mL, and then loaded onto a 5 mL HiTrap Q HP anion exchange column connected to an NGC Chromatography System (BioRad) and washed with water. The $Cj1438_N$-catalyzed reaction product **8a** is neutral, so it was eluted in the wash step. The flow-through fractions were collected (5.0 mL each) and analyzed using mass spectrometry (Thermo Scientific Q Exactive Focus mass spectrometer). Fractions 2, 3, and 4 contained compound **8a**. The purest fractions (2 and 3) were pooled, lyophilized, dissolved in D_2O, and analyzed using mass spectrometry and ^{1}H NMR spectroscopy. Product **9** from the reaction of substrates **3** and **6** was also identified and purified using the same procedures as that for product **8a**.

Identification of Additional $Cj1438_N$-Catalyzed Products. The $Cj1438_N$-catalyzed reaction products **11a** and **11b** were obtained from the incubation of substrate **3** with acceptor substrates **10a** and **10b**, respectively. The reaction conditions were the same as that for producing product **8a**, and the products were identified and purified using the same procedures as that for product **8a**.

Reaction Rate Determinations for $Cj1438_N$ and $Cj1434_N$. The initial rates of the $Cj1438_N$-catalyzed reactions were determined using a HiTrap Q HP anion exchange column to monitor the formation of UDP. $Cj1438_N$ (40 μM) was incubated with substrate **3** (2.0 mM) and acceptor substrate **5a** (4.0 mM) in 50 mM NH_4HCO_3, pH 8.0, at 25 °C. An aliquot of the reaction mixture was heated at 100 °C for 60 s to quench the reaction at different time intervals. The precipitated protein was removed by centrifugation, and the supernatant fluid was passed through a 10K Nanosep spin filter (PALL), diluted in H_2O, and then loaded to a 1.0 mL HiTrap Q HP anion exchange column. The column was connected to an NGC chromatography system (BioRad) (high-performance liquid chromatography) and washed with H_2O. Substrate **3** and the product UDP were cleanly separated by ion exchange chromatography. The initial rate of the $Cj1438_N$-catalyzed reaction was obtained based on the change in UDP concentration as a function of time. The catalytic reaction rate of $Cj1438_N$ using substrate **3** as the donor substrate and acceptor substrates **6** and **10a** was also determined using the same procedures as described above for product **8a**. The reaction rates for the $Cj1434_N$-catalyzed reactions were

https://doi.org/10.1021/acs.biochem.4c00704
Biochemistry 2025, 64, 591−599

determined using the same procedures as those adopted for $Cj1438_N$ except that the concentration of $Cj1434_N$ used for substrate **10a** was 2.0 μM.

RESULTS AND DISCUSSION

Search for Polymerizing Glycosyltransferases from *C. jejuni*. Within the gene cluster for the biosynthesis of the capsular polysaccharide in *C. jejuni*, serotype HS:2 (Figure S2), there are seven putative glycosyltransferases that could facilitate the biosynthesis of the CPS shown in Figure 1. Cj1431 was previously shown via genetic knockout experiments to be responsible for the transfer of D-*glycero*-L-*gluco*-heptose to the D-glucuronic acid moiety.[43] We have shown previously that the N-terminal domain of Cj1432 is responsible for the transfer of D-GlcA from UDP-D-GlcA to the C2-hydroxyl group of D-ribose at the nonreducing end of the growing polysaccharide chain.[40] We have also speculated that the C-terminal domain of Cj1432 is required for the transfer of D-ribose-5-P from phosphoribosyl pyrophosphate to the C5-hydroxyl group of Gal*f*NAc.[40,44] However, the enzyme required for the transfer of D-Gal*f*NAc from UDP-Gal*f*NAc to the C4-hydroxyl group of the D-GlcA moiety of the growing polysaccharide is not known. Of the four remaining glycosyltransferases, the two enzymes most likely to catalyze this reaction are embedded in multidomain proteins Cj1438 and Cj1434.

Deconstruction of Cj1438. The three-dimensional structure of Cj1438 was predicted using AlphaFold2 and is presented in Figure 3.[42] Cj1438 is composed of three

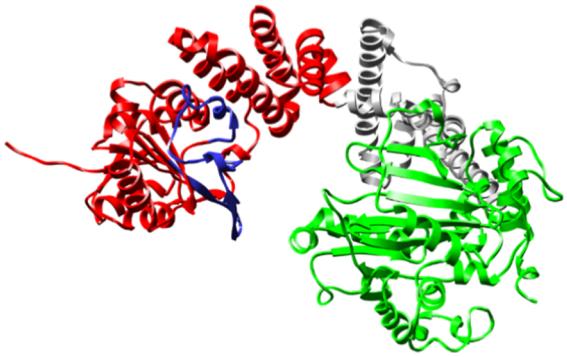

Figure 3. Predicted structure of Cj1438 using AlphaFold2.[42] The red N-terminal domain is annotated to be a GT2 glycosyltransferase, and it extends from residues 1 to 325. The green C-terminal domain adopts a TupA-like ATP-grasp structural fold and extends from residues 453 through 776. These two domains are connected by a third domain colored gray (residues 326−452). The blue colored segment within the red colored domain represents the most diverged segment relative to that found within $Cj1434_N$.

individual domains. The N-terminal domain (colored red and now denoted as $Cj1438_N$) comprises residues 1−325 and is functionally annotated as a GT2 glycosyltransferase by the CAZy database, and as a GT2 glycosyltransferase, it is expected to catalyze its reaction with inversion of configuration at C1 of the donor sugar.[45] The C-terminal domain (colored green), which comprises residues 453−776, has a TupA-like ATP-grasp structural fold and has been shown previously by us to catalyze amide bond formation using the C6-carboxylate of the GlcA moiety and is denoted as $Cj1438_C$.[38,39] These two domains are connected to one another by a third domain (residues 326−452) of unknown function (colored gray in Figure 3). Based on these observations, attempts were made to express the N-terminal domain of Cj1438 via the utilization of a plasmid containing only the codons for the first 325 amino acids and an N-terminal polyhistidine purification tag. $Cj1438_N$ was readily purified after heterologous expression in *E. coli*.

Catalytic Properties of $Cj1438_N$. To test the proposal that the N-terminal domain of Cj1438 is responsible for the transfer of D-Gal*f*NAc to the growing polysaccharide chain, we incubated UDP-D-Gal*f*NAc (**3**) with a variety of possible acceptor substrates. These compounds included the α-methyl glycoside of D-glucuronic acid (**4a**) and three different amidated derivatives (**5a**, **6**, and **7a**). In this initial test of catalytic activity, only compounds **5a** and **6** were substrates for $Cj1438_N$, forming products **8a** and **9**, respectively. The ESI mass spectra of the two isolated products are shown in Figure 4. The ESI-MS of product **9** (Figure 4a) exhibits *m*/*z* ratios of

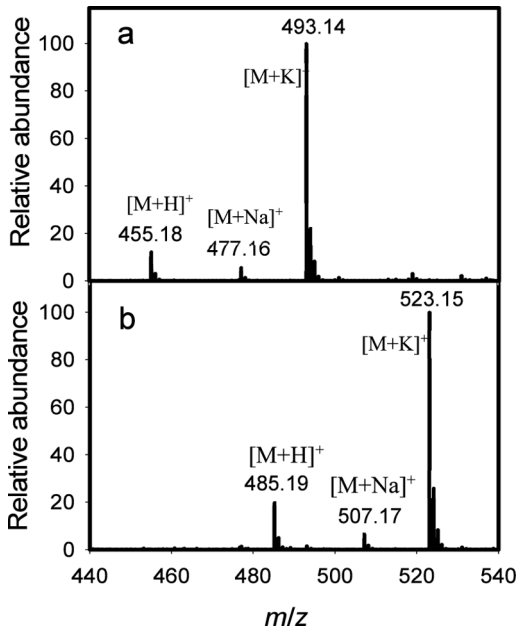

Figure 4. ESI mass spectra of products **8a** and **9** made from the catalytic activity of $Cj1438_N$ with acceptor substrates **5a** and **6** using UDP-D-Gal*f*NAc (**3**) as the donor substrate. (a) ESI−MS of product **9**. (b) ESI−MS of product **8a**.

455.16, 477.16, and 493.10 for the $[M + H]^+$, $[M + Na]^+$, and $[M + K]^+$ ions, respectively, which match the calculated masses for these ions. For product **8a**, the ESI-MS (Figure 4b) exhibits *m*/*z* ratios of 485.19, 507.17, and 523.15 for the $[M + H]^+$, $[M + Na]^+$, and $[M + K]^+$ ions, respectively. These results demonstrate that $Cj1438_N$ catalyzes the transfer of D-Gal*f*NAc to the growing polysaccharide chain and that the D-GlcA moiety must be amidated prior to glycosyl transfer from UDP-D-Gal*f*NAc. The HSQC NMR spectrum of product **8a** is presented in Figure S3.

To establish that the glycosidic bond between the D-glucuronamide and the D-Gal*f*NAc moieties catalyzed by $Cj1438_N$ occurs with the hydroxyl group at C4 of the D-glucuronamide acceptor, the reaction was repeated with substrate **5b**, which contains a ^{13}C-label at C4. Compound **5b** was enzymatically synthesized starting from compound **4b** as summarized in Scheme 1. Unfortunately, the methyl-D-glucuronic acid, **4b**, was isolated as a mixture of the α- and β-anomers in the ratio of 70:30, and this distribution of the two

https://doi.org/10.1021/acs.biochem.4c00704
Biochemistry 2025, 64, 591−599

Scheme 1. Enzymatic Preparation of ^{13}C-Labeled Disaccharide 8b

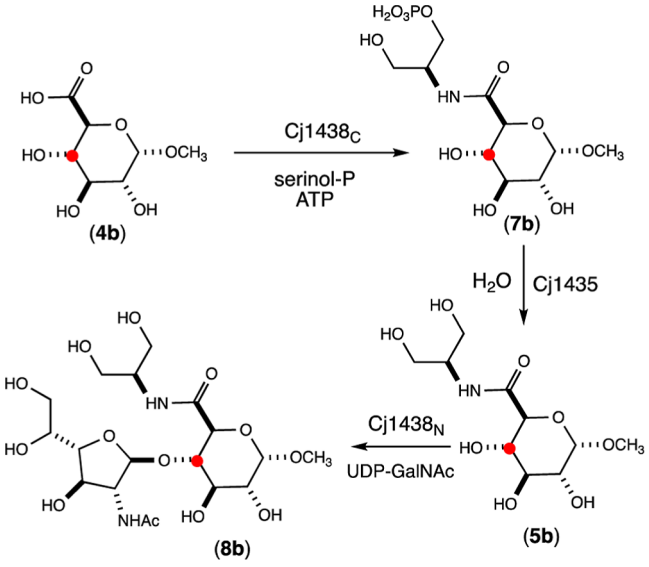

diastereomers is carried through in the enzymatically prepared **5b**. Compound **5b** was used with UDP-D-Gal*f*NAc in the presence of Cj1438$_N$ to prepare ^{13}C-labeled disaccharide **8b**. Portions of the ^{1}H NMR spectra of the substrates and products showing the resonances for the anomeric hydrogens are presented in Figure 5. The anomeric proton for the α-anomer

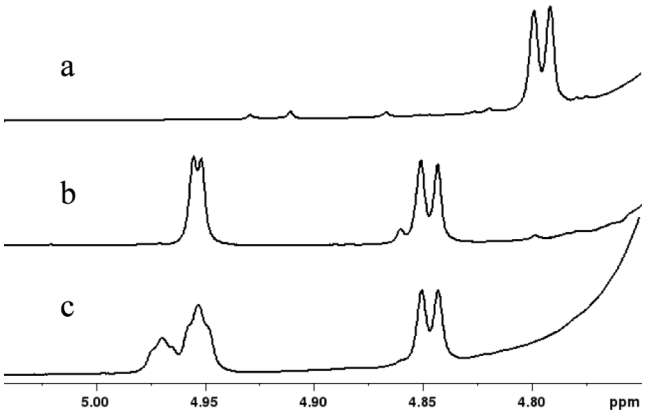

Figure 5. Portions of the NMR spectra for compounds **4b**, **8a**, and **8b** that highlight the resonances for the anomeric hydrogens. (a) Compound **4b**; (b) compound **8a**; (c) compound **8b**. Additional details are provided in the text.

of the substrate **4b** resonates at 4.795 ppm, whereas the β-anomer (not shown) resonates at 4.350 ppm (Figure 5a). The unlabeled disaccharide **8a** exhibits resonances for the two anomeric hydrogens at 4.845 and 4.950 ppm. The doublet at 4.845 ppm originates from the D-glucuronamide moiety, while the doublet at 4.950 ppm is from the D-Gal*f*NAc moiety (Figure 5b). For the ^{13}C-labeled product **8b**, the doublet for the anomeric hydrogen from the D-glucuronamide moiety is also observed at 4.845 ppm, while the resonance for the anomeric hydrogen from the GalNAc moiety is now an unresolved triplet at 4.950 ppm owing to the additional $^3J_{H-C}$ coupling to the ^{13}C-label at C4 of the glucuronamide moiety. The additional triplet at 4.970 ppm originates from the β-anomer. These results establish that the reaction catalyzed by Cj1438$_N$ occurs with the C4 hydroxyl of the glucuronamide acceptor substrate.

To further elaborate the catalytic properties of Cj1438$_N$, we tested this enzyme using D-ribose-D-glucuronamide disaccharides (**10a** and **10b**) as acceptor substrates to make trisaccharide products **11a** and **11b** (Scheme 2). Disaccharide

Scheme 2. Reaction of Substrates 10a and 10b and UDP-GalNAc Catalyzed by Cj1438$_N$

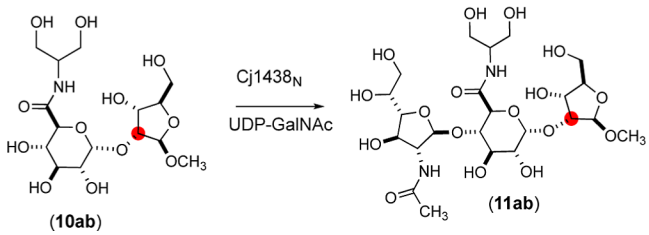

10b contains a ^{13}C-label at C2 within the D-ribose moiety of this substrate. The disaccharides **10a** and **10b** were excellent substrates for Cj1438$_N$, and the ESI mass spectra of the isolated products are presented in Figure 6. Product **11a**

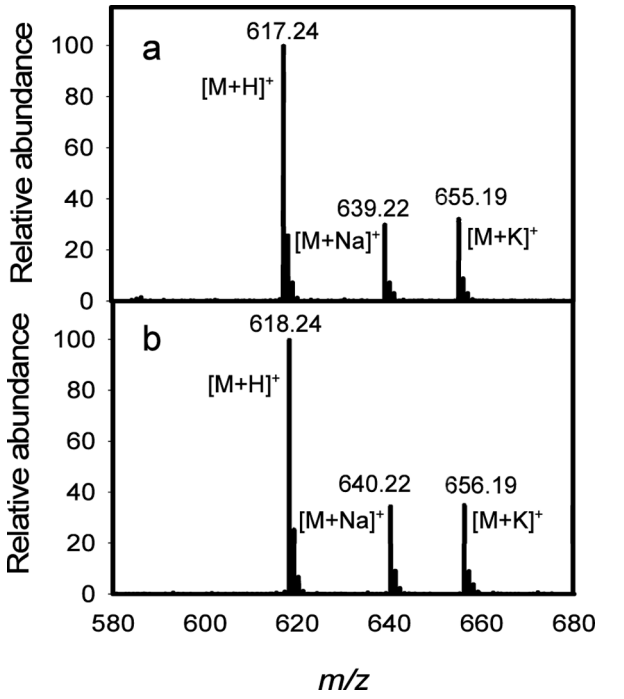

Figure 6. ESI−MS of products **11a** and **11b** made from the catalytic activity of Cj1438$_N$ with acceptor substrates **10a** and **10b** using UDP-GalNAc (**3**) as the donor substrate. (a) ESI−MS of product **11a**. (b) ESI−MS of product **11b**.

exhibits *m*/*z* ratios of 617.24, 639.22, and 655.19, for the $[M + H]^+$, $[M + Na]^+$, and $[M + K]^+$ complexes, respectively, which matched the calculated masses for these complexes. The ^{13}C-labeled product **11b** exhibited *m*/*z* ratios of 618.24, 640.22, and 656.19 for the $[M + H]^+$, $[M + Na]^+$, and $[M + K^+]^+$ complexes that matched the expected values (Figure 6b).

Deconstruction of Cj1434. The GT2 glycosyltransferase Cj1434 is also a potential enzyme for the formation of a glycosidic bond between the D-GlcA and D-Gal*f*NAc moieties in the CPS of *C. jejuni*. The AlphaFold2-predicted structure of

https://doi.org/10.1021/acs.biochem.4c00704
Biochemistry 2025, 64, 591−599

this enzyme is presented in Figure 7, where the first 327 residues are colored magenta and the C-terminal domain

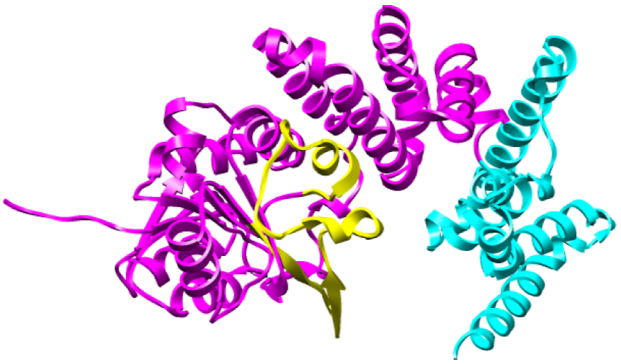

Figure 7. AlphaFold2-predicted structure of Cj1434. The N-terminal domain is highlighted in magenta and the C-terminal domain highlighted in cyan. The portion of the protein that differs most in sequence with the N-terminal domain of Cj1438 is highlighted in yellow.

(residues 328−445) is shown in cyan. Curiously, the N-terminal domains of Cj1438 (residues 1−325) and Cj1434 (residues 1−327) are 87% identical in amino acid sequence (see Figure S4), suggesting that both enzymes will catalyze the same (or very similar) reactions. In Figure 8, a structural

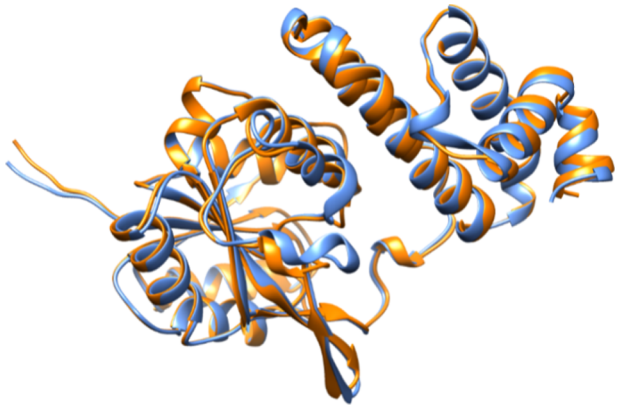

Figure 8. Structural alignment of the N-terminal domains of Cj1438 (orange) and Cj1434 (blue).

alignment of the N-terminal domains of Cj1434 and Cj1438 is presented, which illustrates the clear similarity in the two folded structures. We first attempted to express the gene for the entire sequence of Cj1434 but were unable to obtain soluble protein. Therefore, we obtained a plasmid that was limited to the expression for the first 327 amino acid residues. This protein was purified and subsequently denoted as $Cj1434_N$.

The largest section of divergence in the amino acid sequences between $Cj1434_N$ and $Cj1438_N$ extends from residues 126 to 159, and these sections of the two proteins are highlighted in blue for Cj1438 in Figure 3 and in yellow for Cj1434 (Figure 7). Structural alignments of $Cj1434_N$ and $Cj1438_N$ with the N-terminal domain of the GT2 glycosyltransferase TarS from *Staphylococcus aureus* (PDB id: 5TZJ) bound with the donor substrate UDP-GlcNAc are presented in Figure S5. The predicted distances from C1 of the bound GlcNAc to the α-carbons of residues 126−159 in these two structural comparisons range from 14 to 29 Å. Therefore, this region of the two proteins is not involved **in** the binding of the sugar donor, UDP-Gal*f*NAc, but may contribute to the binding of an extended polysaccharide acceptor.

Catalytic Properties of Cj1434N. The catalytic activities of $Cj1434_N$ were found to be the same as that determined for $Cj1438_N$. Using UDP-D-Gal*f*NAc (**3**) as the sugar donor, $Cj1434_N$ was demonstrated to convert substrates **5a**, **6**, **10a**, and **10b** to products **8a**, **9**, **11a**, and **11b**, respectively. The ESI-MS results of the isolated products are presented in Figure S6.

Reaction Rates for Catalysis by $Cj1438_N$ and $Cj1434_N$. The reaction rates for $Cj1438_N$ were determined by using a HiTrap Q HP anion exchange column to measure the rate of formation of UDP as a function of time. $Cj1438_N$ was incubated with donor substrate **3** (2.0 mM) and various acceptor substrates **5a**, **6**, and **10a** (4.0 mM). The reactions were quenched by denaturing the protein at different time intervals. The initial reaction rates using donor substrate **3** with acceptor substrates **5a**, **6**, and **10a** were determined to be 0.66 ± 0.05, 0.59 ± 0.02, and 1.14 ± 0.06 min^{-1}, respectively. The reaction rates of $Cj1434_N$ were determined using the same conditions and procedures as that for $Cj1438_N$. The reaction rates of $Cj1434_N$ using donor substrate **3** and acceptor substrates **5a**, **6**, and **10a** were determined to be 5.9 ± 0.3, 3.7 ± 0.2, and 204 ± 18 min^{-1}, respectively. The time courses for product formation as a function of time are presented in Figure S7. Under these conditions, $Cj1434_N$ is a better catalyst than $Cj1438_N$.

Previously, we demonstrated that the N-terminal domain of Cj1432 was able to catalyze the transfer of GlcA from UDP-GlcA to an acceptor D-ribofuranoside at C2 with retention of the configuration (40). In this report, we demonstrate that the N-terminal domains of either Cj1438 or Cj1434 can catalyze the transfer of Gal*f*NAc from UDP-Gal*f*NAc to a modified D-glucuronic acid acceptor substrate that must first be amidated with either serinol or ethanolamine. The amidation of the D-GlcA moiety has previously been shown to be catalyzed by the C-terminal domain of Cj1438 using ATP and either (*S*)-serinol-P or ethanolamine-P.[39] The phosphoryl group is subsequently hydrolyzed by Cj1435.[38] The collective reactions catalyzed by the two glycosyltransferases and the three auxiliary enzymes for the biosynthesis of the unique trisaccharide are summarized in Figure 9.

It is not at all clear why there are two enzymes that catalyze the transfer of Gal*f*NAc from UDP-D-Gal*f*NAc to the C4-hydroxyl group of the D-glucuronamide moiety of the growing carbohydrate chain. However, a similar situation is found in the gene cluster for the biosynthesis of the HS:19 serotype of *C. jejuni* (Figure S8). The CPS from the HS:19 serotype (compound **2**, Figure 1) is composed of a repeating disaccharide sequence of D-GlcNAc and the serinol amide of D-glucuronic acid.[33] The C-terminal domain of HS19.11 (UniProt id: Q5M6M2) is homologous (61% identical) to the amidoligase domain from the C-terminal end of Cj1438 from HS:2 (Figure S9). The glycosyltransferase at the N-terminal domain of HS19.11 (now predicted to catalyze the transfer of D-GlcNAc from UDP-D-GlcNAc to the serinol amide of D-glucuronic acid) is 67% identical to the glycosyltransferase found in the N-terminal domain of HS19.08 (Figure S10).

We have now been able to characterize two different polymerizing glycosyltransferases ($Cj1432_N$ and $Cj1438_N$/

https://doi.org/10.1021/acs.biochem.4c00704
Biochemistry 2025, 64, 591−599

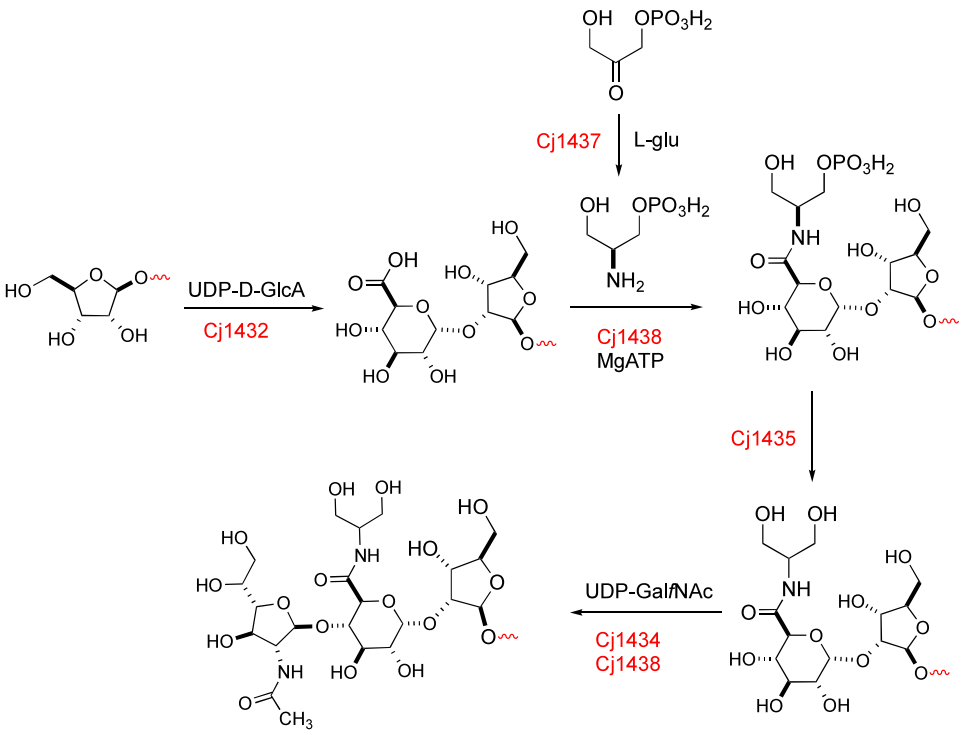

Figure 9. Summary of the reactions catalyzed by Cj1432, Cj1434, Cj1435, Cj1437, and Cj1438 during the biosynthesis of the capsular polysaccharide of the HS:2 serotype of *C. jejuni*..

Cj1434$_N$) from the HS:2 serotype of *C. jejuni*, and this has enabled the chemoenzymatic synthesis of a trisaccharide composed of D-Gal*f*NAc-D-GlcA-D-Rib (product **11a**). The remaining polymerizing glycosyltransferase, needed for the attachment of D-ribose, will ultimately allow for the chemoenzymatic synthesis of the other two possible trisaccharides (D-Rib-D-Gal*f*NAc-D-GlcA and D-GlcA-D-Rib-D-Gal*f*NAc) in addition to the synthesis of much longer repeating polysaccharides. The characterization of the third polymerizing glycosyltransferase is in progress.

CONCLUSIONS

The exterior surface of the human pathogen *C. jejuni* is coated with a capsular polysaccharide that helps to protect it from the host immune response. Different strains and serotypes of the bacterium synthesize unique and variable sequences of carbohydrates for the CPS. In the HS:2 serotype from *C. jejuni* NCTC 11168, the CPS is composed of a repeating sequence of D-ribose, *N*-acetyl-D-galactosamine, and D-glucuronic acid. The D-glucuronic acid moiety is further decorated by amidation with serinol and glycosylation with D-*glycero*-L-*gluco*-heptose. We identified two enzymes (Cj1438 and Cj1434) capable of catalyzing the transfer of *N*-acetyl-D-galactosamine from UDP-Gal*f*NAc to the C4-hydroxyl group of the D-glucuronamide moiety at the nonreducing end of the growing CPS. These results clearly demonstrate that after D-glucuronic acid has been added to the nonreducing end of the CPS, it must be first amidated with either serinol or ethanolamine by the catalytic activities of Cj1438 and Cj1435 prior to the addition of Gal*f*NAc. Cj1438 and Cj1434 are multidomain proteins, and the GT2 glycosyltransferase activities are located within the N-terminal half of these complex enzymes.

ASSOCIATED CONTENT

Supporting Information

The Supporting Information is available free of charge at https://pubs.acs.org/doi/10.1021/acs.biochem.4c00704.

Amino acid sequences of the purified proteins, protein sequence comparisons, and NMR spectra of chemically synthesized substrates and enzyme-catalyzed reaction products (PDF)

Accession Codes

Accession codes: Cj1438 (UniProt id: Q0P8H6) Cj1434 (UniProt id: Q0P8I0)

AUTHOR INFORMATION

Corresponding Author

Frank M. Raushel − *Department of Chemistry, Texas A&M University, College Station, Texas 77842, United States;* orcid.org/0000-0002-5918-3089; Email: raushel@tamu.edu

Authors

Dao Feng Xiang − *Department of Chemistry, Texas A&M University, College Station, Texas 77842, United States*

Tamari Narindoshvili − *Department of Chemistry, Texas A&M University, College Station, Texas 77842, United States*

Complete contact information is available at: https://pubs.acs.org/10.1021/acs.biochem.4c00704

Funding

This research was supported by the National Institutes of Health (GM 139428).

Notes

The authors declare no competing financial interest.

REFERENCES

(1) Elmi, A.; Nasher, F.; Dorrell, N.; Wren, B.; Gundogdu, O. Revisiting *Campylobacter jejuni* Virulence and Fitness Factors: Role in Sensing, Adapting, and Competing. *Front. Cell. Infect. Microbiol.* **2021**, *10*, 607704.

(2) Chantzaras, A. P.; Karageorgos, S.; Panagiotou, P.; Georgiadou, E.; Chousou, T.; Spyridopoulou, K.; Paradeisis, G.; Kanaka-Gantenbein, C.; Botsa, E. Myocarditis in a Pediatric Patient with *Campylobacter* Enteritis: A Case Report and Literature Review. *Trop Med. Infect Dis* **2021**, *6*, 212.

(3) Nachamkin, I.; Allos, B. M.; Ho, T. *Campylobacter* Species and Guillain-Barré Syndrome. *Clin. Microbiol. Rev.* **1998**, *11*, 555−567.

(4) Tikhomirova, A.; McNabb, E. R.; Petterlin, L.; Bellamy, G. L.; Lin, K. H.; Santoso, C. A.; Daye, E. S.; Alhaddad, F. M.; Lee, K. P.; Roujeinikova, A. *Campylobacter jejuni* Virulence Factors: Update on Emerging Issues and Trends. *J. Biomed. Sci.* **2024**, *31*, 45.

(5) Thépault, A.; Rose, V.; Queguiner, M.; Chemaly, M.; Rivoal, K. Dogs and Cats: Reservoirs for Highly Diverse *Campylobacter jejuni* and a Potential Source of Human Exposure. *Animals* **2020**, *10*, 838.

(6) Dessouky, Y. E.; Elsayed, S. W.; Abdelsalam, N. A.; Saif, N. A.; Álvarez-Ordóñez, A.; Elhadidy, M. Genomic Insights into Zoonotic Transmission and Antimicrobial Resistance in *Campylobacter jejuni* from Farm to Fork: A One Health Perspective. *Gut Pathog.* **2022**, *14*, 44.

(7) Riddle, M. S.; Guerry, P. Status of Vaccine Research and Development for *Campylobacter jejuni*. *Vaccine* **2016**, *34*, 2903−2906.

(8) Guerry, P.; Poly, F.; Riddle, M.; Maue, A. C.; Chen, Y.-H.; Monteiro, M. A. *Campylobacter* Polysaccharide Capsules: Virulence and Vaccines. *Front. Cell. Infect. Microbiol.* **2012**, *2*, 7.

(9) van Alphen, L. B.; Wenzel, C. Q.; Richards, M. R.; Fodor, C.; Ashmus, R. A.; Stahl, M.; Karlyshev, A. V.; Wren, B. W.; Stintzi, A.; Miller, W. G.; Lowary, T. L.; Szymanski, C. M. Biological Roles of the O-methyl Phosphoramidate Capsule Modification in *Campylobacter jejuni*. *PLoS One* **2014**, *9*, No. e87051.

(10) Monteiro, M. A.; Noll, A.; Laird, R. M.; Pequegnat, B.; Ma, Z. C.; Bertolo, L.; DePass, C.; Omari, E.; Gabryelski, P.; Redkyna, O.; Jiao, Y. N.; Borrelli, S.; Poly, F.; Guerry, P. *Campylobacter jejuni* Capsule Polysaccharide Conjugate Vaccine. In *Carbohydrate-based Vaccines: From Concept to Clinic*; American Chemical Society: Washington, DC, 2018; pp 249−271.

(11) Aspinall, G. O.; McDonald, A. G.; Pang, H.; Kurjanczyk, L. A.; Penner, J. L. Lipopolysaccharides of *Campylobacter jejuni* Serotype O:19: Structures of Core Oligosaccharide Regions from the Serostrain and Two Bacterial Isolates from Patients with the Guillain-Barré Syndrome. *Biochemistry* **1994**, *33*, 241−249.

(12) Aspinall, G. O.; McDonald, A. G.; Pang, H. Lipopolysaccharides of *Campylobacter jejuni* Serotype O:19: Structures of O Antigen Chains from the Serostrain and Two Bacterial isolates from patients with the Guillain-Barré syndrome. *Biochemistry* **1994**, *33*, 250−255.

(13) McNally, D. J.; Jarrell, H. C.; Khieu, N. H.; Li, J.; Vinogradov, E.; Whitfield, D. M.; Szymanski, C. M.; Brisson, J. R. The HS:19 serostrain of *Campylobacter jejuni* has a Hyaluronic Acid-type Capsular Polysaccharide with a Nonstoichiometric Sorbose Branch and O-methyl Phosphoramidate Group. *FEBS J.* **2006**, *273*, 3975−3989.

(14) Michael, F. S.; Szymanski, C. M.; Li, J. J.; Chan, K. H.; Khieu, N. H.; Larocque, S.; Wakarchuk, W. W.; Brisson, J. R.; Monteiro, M. A. The Structures of the Lipooligosaccharide and Capsule Polysaccharide of *Campylobacter jejuni* Genome Sequenced Strain NCTC 11168. *Eur. J. Biochem.* **2002**, *269*, 5119−5136.

(15) Butty, F. D.; Aucoin, M.; Morrison, L.; Ho, N.; Shaw, G.; Creuzenet, C. Elucidating the Formation of 6-Deoxyheptose: Biochemical Characterization of the GDP-D-*glycero*-D-*manno*-heptose C6 Dehydratase, DmhA, and its Associated C4 Reductase, DmhB. *Biochemistry* **2009**, *48*, 7764−7775.

(16) McCallum, M.; Shaw, G. S.; Creuzenet, C. Characterization of the Dehydratase WcbK and the Reductase WcaG Involved in GDP-6-deoxy-*manno*-heptose Biosynthesis in *Campylobacter jejuni*. *Biochem. J.* **2011**, *439*, 235−248.

(17) McCallum, M.; Shaw, S. D.; Shaw, G. S.; Creuzenet, C. Complete 6-Deoxy-D-*altro*-heptose Biosynthesis Pathway from *Campylobacter jejuni*: More Complex than Anticipated. *J. Biol. Chem.* **2012**, *287*, 29776−29788.

(18) McCallum, M.; Shaw, G. S.; Creuzenet, C. Comparison of Predicted Epimerases and Reductases of the *Campylobacter jejuni* D-*altro*- and L-*gluco*-Heptose Synthesis Pathways. *J. Biol. Chem.* **2013**, *288*, 19569−19580.

(19) Barnawi, H.; Woodward, L.; Fava, N.; Roubakha, M.; Shaw, S. D.; Kubinec, C.; Naismith, J. H.; Creuzenet, C. Structure-function Studies of the C_3/C_5 Epimerases and C_4 Reductases of the *Campylobacter jejuni* Capsular Heptose Modification Pathways. *J. Biol. Chem.* **2021**, *296*, 100352.

(20) Huddleston, J. P.; Raushel, F. M. Biosynthesis of GDP-D-glycero-α-D-manno-heptose for the Capsular Polysaccharide of *Campylobacter jejuni*. *Biochemistry* **2019**, *58*, 3893−3902.

(21) Huddleston, J. P.; Anderson, T. K.; Girardi, N. M.; Thoden, J. B.; Taylor, Z.; Holden, H. M.; Raushel, F. M. Biosynthesis of D-Glycero-L-gluco-heptose in the Capsular Polysaccharides of *Campylobacter jejuni*. *Biochemistry* **2021**, *60*, 1552−1563.

(22) Huddleston, J. P.; Anderson, T. K.; Spencer, K. D.; Thoden, J. B.; Raushel, F. M.; Holden, H. M. Structural analysis of Cj1427, an Essential NAD-dependent Dehydrogenase for the Biosynthesis of the Heptose Residues in the Capsular Polysaccharides of *Campylobacter jejuni*. *Biochemistry* **2020**, *59*, 1314−1327.

(23) Huddleston, J. P.; Raushel, F. M. Functional Characterization of Cj1427, a Unique Ping-pong Dehydrogenase Responsible for the Oxidation of GDP-D-glycero-α-D-manno-heptose in *Campylobacter jejuni*. *Biochemistry* **2020**, *59*, 1328−1337.

(24) Poulin, M. B.; Shi, Y.; Protsko, C.; Dalrymple, S. A.; Sanders, D. A. R.; Pinto, B. M.; Lowary, T. L. Specificity of a UDP-GalNAc Pyranose-furanose Mutase: A Potential Therapeutic Target for *Campylobacter jejuni* Infections. *ChemBioChem* **2014**, *15*, 47−56.

(25) Xiang, D. F.; Thoden, J. B.; Ghosh, M. K.; Holden, H. M.; Raushel, F. M. Reaction Mechanism and Three-dimensional Structure of GDP-glycero-α-D-manno-heptose 4, 6-Dehydratase from *Campylobacter jejuni*. *Biochemistry* **2022**, *61*, 1313−1322.

(26) Ghosh, M. K.; Xiang, D. F.; Thoden, J. B.; Holden, H. M.; Raushel, F. M. C3- and C3/C5-Epimerases Required for the Biosynthesis of the Capsular Polysaccharides from *Campylobacter jejuni*. *Biochemistry* **2022**, *61*, 2036−2048.

(27) Ghosh, M. K.; Xiang, D. F.; Raushel, F. M. Product Specificity of the C4-Reductases in the Biosynthesis of GDP-6-deoxy-heptoses During Capsular Polysaccharide Formation in *Campylobacter jejuni*. *Biochemistry* **2022**, *61*, 2138−2147.

(28) Simons, M. E.; Narindoshvili, T.; Raushel, F. M. Biosynthesis of UDP-β-L-Arabinofuranoside for the Capsular Polysaccharides of *Campylobacter jejuni*. *Biochemistry* **2023**, *62*, 3012−3019.

(29) Xiang, D. F.; Ghosh, M. K.; Riegert, A. S.; Thoden, J. B.; Holden, H. M.; Raushel, F. M. Bifunctional Epimerase/Reductase Enzymes Facilitate the Modulation of 6-Deoxy-Heptoses Found in the Capsular Polysaccharides of *Campylobacter jejuni*. *Biochemistry* **2023**, *62*, 134−144.

(30) Ghosh, M. K.; Xiang, D. F.; Raushel, F. M. Biosynthesis of 3, 6-Dideoxy-heptoses for the Capsular Polysaccharides of *Campylobacter jejuni*. *Biochemistry* **2023**, *62*, 1287−1297.

(31) Xiang, D. F.; Xu, M.; Ghosh, M. K.; Raushel, F. M. Metabolic Pathways for the Biosynthesis of Heptoses Used in the Construction of Capsular Polysaccharides in the Human Pathogen *Campylobacter jejuni*. *Biochemistry* **2023**, *62*, 3145−3158.

(32) Ghosh, M. K.; Narindoshvili, T.; Thoden, J. B.; Schumann, M. E.; Holden, H. M.; Raushel, F. M. Biosynthesis of Cytidine Diphosphate-6-D-Glucitol for the Capsular Polysaccharides of *Campylobacter jejuni*. *Biochemistry* **2024**, *63*, 699−710.

(33) Ghosh, M. K.; Raushel, F. M. Biosynthesis of UDP-α-N-Acetyl-D-mannosaminuronic Acid and CMP-β-N-Acetyl-D-neuraminic Acid for the Capsular Polysaccharides of *Campylobacter jejuni*. *Biochemistry* **2024**, *63*, 688−698.

https://doi.org/10.1021/acs.biochem.4c00704
Biochemistry 2025, 64, 591−599

(34) Taylor, Z. W.; Raushel, F. M. Manganese-Induced Substrate Promiscuity in the Reaction Catalyzed by Phosphoglutamine Cytidylyltransferase from *Campylobacter jejuni*. *Biochemistry* **2019**, *58*, 2144−2151.
(35) Taylor, Z. W.; Chamberlain, A. R.; Raushel, F. M. Substrate Specificity and Chemical Mechanism for the Reaction Catalyzed by Glutamine Kinase. *Biochemistry* **2018**, *57*, 5447−5455.
(36) Taylor, Z. W.; Raushel, F. M. Cytidine Diphosphoramidate Kinase: An Enzyme Required for the Biosynthesis of the O-Methyl Phosphoramidate Modification in the Capsular Polysaccharides of *Campylobacter jejuni*. *Biochemistry* **2018**, *57*, 2238−2244.
(37) Riegert, A. S.; Narindoshvili, T.; Coricello, A.; Richards, N. G. J.; Raushel, F. M. Functional Characterization of Two PLP-Dependent Enzymes Involved in Capsular Polysaccharide Biosynthesis from *Campylobacter jejuni*. *Biochemistry* **2021**, *60*, 2836−2843.
(38) Riegert, A. S.; Narindoshvili, T.; Platzer, N. E.; Raushel, F. M. Functional Characterization of a HAD Phosphatase Involved in Capsular Polysaccharide Biosynthesis in *Campylobacter jejuni*. Biochemistry. *Biochemistry* **2022**, *61*, 2431−2440.
(39) Riegert, A. S.; Narindoshvili, T.; Raushel, F. M. Discovery and Functional Characterization of a Clandestine ATP-Dependent Amidoligase in the Biosynthesis of the Capsular Polysaccharide from *Campylobacter jejuni*. *Biochemistry* **2022**, *61*, 117−124.
(40) Xiang, D. F.; Riegert, A. S.; Narindoshvili, T.; Raushel, F. M. Identification of the Polymerizing Glycosyltransferase Required for the Addition of D-Glucuronic Acid to the Capsular Polysaccharide of *Campylobacter jejuni*. *Biochemistry* **2025**, *64*, DOI: 10.1021/acs.biochem.4c00703.
(41) Gasteiger, E.; Hoogland, C.; Gattiker, A.; Duvaud, S. E.; Bairoch, A. Protein Identification and Analysis Tools on the ExPASy Server. In *The Proteomics Protocols Handbook*; Walker, J. M., Ed.; Humans Press: Totowa, NJ, 2005; pp 571−607.
(42) Jumper, J.; Evans, R.; Pritzel, A.; Green, T.; Figurnov, M.; Ronneberger, O.; Tunyasuvunakool, K.; Bates, R.; Žídek, A.; Potapenko, A.; Bridgland, A.; Meyer, C.; Kohl, S. A. A.; Ballard, A. J.; Cowie, A.; Romera-Paredes, B.; Nikolov, S.; Jain, R.; Adler, J.; Back, T.; Petersen, S.; Reiman, D.; Clancy, E.; Zielinski, M.; Steinegger, M.; Pacholska, M.; Berghammer, T.; Bodenstein, S.; Silver, D.; Vinyals, O.; Senior, A. W.; Kavukcuoglu, K.; Kohli, P.; Hassabis, D. Highly Accurate Protein Structure Prediction with AlphaFold. *Nature* **2021**, *596*, 583−589.
(43) Reid, A. N.; Pandey, R.; Palyada, K.; Whitworth, L.; Doukhanine, E.; Stintzi, A. Identification of *Campylobacter jejuni* Genes Contributing to Acid Adaptation by Transcriptional Profiling and Genome-Wide Mutagenesis. *Appl. Environ. Microbiol.* **2008**, *74*, 1598−1612.
(44) Sternberg, M. J. E.; Tamaddoni-Nezhad, A.; Lesk, V. I.; Kay, E.; Hitchen, P. G.; Cootes, A.; van Alphen, L. B.; Lamoureux, M. P.; Jarrell, H. C.; Rawlings, C. J.; Soo, E. C.; Szymanski, C. M.; Dell, A.; Wren, B. W.; Muggleton, S. H. Gene Function Hypotheses for the *Campylobacter jejuni*. Glycome Generated by a Logic-Based Approach. *J. Mol. Biol.* **2013**, *425*, 186−197.
(45) Drula, E.; Garron, M.-L.; Dogan, S.; Lombard, V.; Henrissat, B.; Terrapon, N. The Carbohydrate-active Enzyme Database: Functions and Literature. *Nucleic Acids Res.* **2022**, *50*, D571−D577.